A Grounded Low-Cost UHF RFID Tag Antenna for Long-Range Metallic and Non-Metallic objects Applications

Mohamed El Amine Lakhal, Mohammed Ali Ennasar, Mohamed EL Khamlichi, Mariem Aznabet, Otman EL Mrabet, and Mohsine Khalladi

Intelligent System Design (ISD) Laboratory, Faculty of Sciences, Abdelmalek Essaadi University, Tétouan, 93000, Morocco

Corresponding author: Mohamed El Amine Lakhal (amine.lakhl@gmail.com).

ABSTRACT This paper presents an ultra-high frequency (UHF) RFID tag antenna designed to operate within the American frequency band (902-928 MHz) and perform reliably when placed on metallic objects. The design features a microstrip dipole antenna with symmetrical U-shaped stubs, capacitively coupled to a metallic patch and grounded with a substrate. The antenna is printed on a low-cost FR4 substrate (1.6 mm thickness), with overall dimensions of 90 mm × 95 mm × 1.6 mm. The antenna achieves a realized gain of -4.8 dB, with a free-space reading range of approximately 7 m, which increases to 10.5 m when placed on a 50 cm× 30 cm metallic plate. The key of this design lies in its use of capacitive coupling, which eliminates the need for metallic vias or shorting walls. This simplification not only facilitates mass production but also enhances the design's performance, offering a superior reading range on larger metallic objects compared to other designs reported in the literature that provide a small reading range. The proposed antenna offers a robust solution for RFID applications on both metallic and non-metallic objects.

INDEX TERMS Conjugate matching, Metallic objects, Read range, Reflection Coefficients, RFID tag antenna.

I. INTRODUCTION

RFID technology [1] takes advantage of electromagnetic fields to transfer data between a RFID tag antenna and a reader. The RFID system consists of three primary components: the RFID tag antenna, which stores information about the object; the reader, which communicates with the tag and captures data; and the middleware, which facilitates the wireless communication by transmitting and receiving signals. The design and configuration of RFID tag antennas play a crucial role in ensuring efficient and reliable communication between tags and readers. In recent years, Radio Frequency Identification (RFID) technology has emerged as a versatile and pervasive solution for various applications in industries such as logistics, retail, healthcare, and transportation [2], [3], [4]. In addition to these applications, RFID technology has also been successfully used recently in sensing applications where the RFID system's capabilities extend beyond identification and tracking to capture additional data about the object or its environment [5], [6], [7], [8]. Frequency bands used in RFID systems vary depending on the application and regional regulations. In the Ultra High Frequency (UHF) band, which spans from 860 MHz to 960 MHz, several frequency ranges have gained prominence in RFID deployments. These include the 860-868 MHz band, which is common in Europe and North Africa, and the 902-928 MHz band, widely used in North America [9], [10], [11]. These UHF bands offer advantages over lower frequency bands (LF and HF) such as longer read ranges, improved penetration through materials, and compatibility with a wide range of RFID devices [12].

Metallic surfaces present unique challenges and opportunities for RFID systems. Designing an RFID tag antenna that operates efficiently on metallic objects introduces specific difficulties, such as detuning the resonant frequency, which can affect the performance of the RFID tag antennas. Additionally, there is an inherent tradeoff between tag antenna size and read range. As the tag antenna size decreases, the read range tends to be decreased. Conversely, larger antennas may provide improved read range but are impractical due to size limitations.

In order to mitigate the impact of the metallic objects on the RFID tag antenna characteristics, some techniques and methods have been proposed over the past two decades. For example, authors in [13] introduced a tag for the UHF band, utilizing a grounded microstrip patch type antenna. Generally, this kind of microstrip technology leads to a final design with large size, where the resonance length nearly equivalent to $\frac{\lambda}{4}$ (where λ is the wavelength). To overcome this problem, some authors introduced other techniques

based on the use of shorting vias or vertical shorting walls to form a grounded dipole type tag antenna [14], [15]. While the effect of metal objects on tag antenna characteristics is reduced, resulting in increasing manufacturing costs and favorable reading performance. The tag antennas typically exhibit either significant physical dimensions or a small reading range. Other authors explored different variations of patch structures such as planar inverted F antenna (PIFA) [16], [17], and its modified versions like the planar inverted-L antenna (PILA) [18], [19] to develop compact RFID tag antenna designs for on metal applications. Flexible high permittivity substrate [20], innovative and advanced materials, such as graphene [21]. However, the application of these innovative materials can increase the fabrication cost. More recently, the Huygens source, which combines an electric and orthogonal magnetic dipoles, has been investigated to tackle the problem of metallic objects and body effect by designing ungrounded RFID tag antennas [22]. An alternative technique that has been introduced, to address the challenges posed by metallic objects, is based on the use of high impedance surface (HIS) such as artificial magnetic conductor (AMC), and electromagnetic band gap (EBG) [23], [24] ,[25]. For example, in [23] the authors proposed a passive RFID tag antenna suitable for a recessed cavity in metallic objects with a long-read range by using an AMC ground plane. However, the whole dimension of this structure is too big, about 140 mm × 80 mm × 50 mm, which is not suitable to be used in many applications.

In this paper, we have proposed a grounded UHF RFID tag antenna for metallic and no metallic objects. The proposed design consists of a loaded dipole with T-matching which is coupled capacitively with a loaded rectangular patch. This design, with a whole dimension of 90 mm × 95 mm × 1.6 mm, has been printed on a FR_4 substrate with a thickness of 1.6 mm. To confirm the simulated outcomes, a prototype is fabricated and tested. The proposed RFID tag antenna provides at 920 MHz a reading range close to 7 m (free space), and close to 10.5 m when mounted on a flat metallic plate (50 cm × 30 cm), respectively.

II. Antenna Design and Analysis

The configuration of the proposed design is depicted in Figure 1. It consists of a T matching feed, a dipole antenna loaded at both sides with U shaped strips, which is a capacitive coupling with the rectangular patch. To increase this capacitive coupling, two microstrip lines have been introduced on either side of the rectangular patch. The RFID tag antenna is printed on a FR_4 substrate having a permittivity of 4.4, loss tangent of 0.002 and a thickness of 1.6 mm.

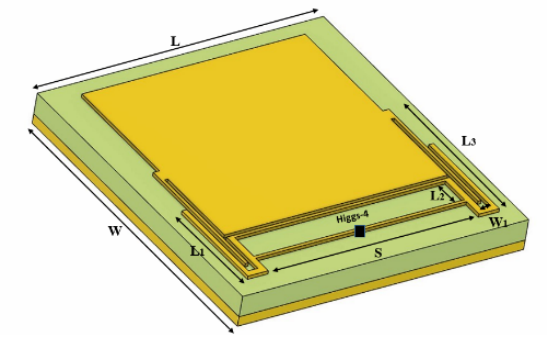

Figure 1: Configuration of the proposed UHF RFID tag antenna with metallic ground

The Higgs 4 RFID chip [26] is connected directly at the center of the T-matching of the antenna structure, the selected IC chip features a reading sensitivity PIC of -20.5 dBm and an input impedance of 18.43 - j183.16 Ω at 920 MHz. The RFID chip has been mounted as depicted in Figure 1. The RFID tag antenna was designed using CST Microwave Studio and optimized to operate within the UHF band, specifically the North American band 902-928 MHz. The input impedance of the proposed design is adjusted by varying the dimensions of the U-shaped strip, the length of the transmission lines, and the rectangular patch dimension. The ultimate optimized parameters values are listed in Table 1. When performing the simulation, the antenna was mounted on a 50 cm x 30 cm perfect electrical conductor (PEC) surface. Notably, the tag performance in terms of reflection coefficient, gain, read range patterns, realized gain, and directivity, or read range. The main feature of this design is the use of capacitive coupling to reduce the size of the proposed design by avoiding short vias or adding separation substrate which leads to a low-profile design, easy, and low-cost fabrication.

Table 1. Optimized dimensions of the RFID tag antenna [mm].

Symbol	Size (mm)
W	95
W_1	3
L	90
L_1	31
L_2	10
L_3	43
S	67

The impedance characteristics of the RFID tag antenna were represented in Figure 2. According to the simulation results, the antenna's input impedance at 920 MHz is (18.52 + j185.6 Ω), which ensures efficient power transfer between the antenna and the Higgs chip (18.43 − j183.16 Ω). This is achieved by ensuring that the antenna impedance is the

complex conjugate of the chip impedance, thereby minimizing reflections and optimizing performance.

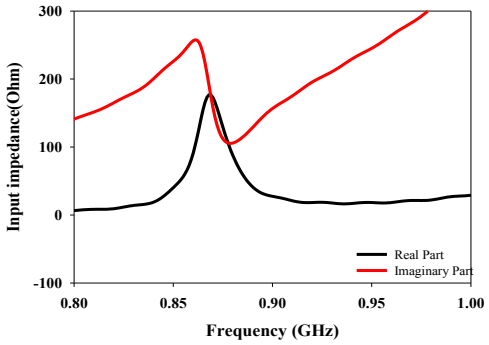

Figure 2: Simulated input impedance of the proposed design in free space.

III. Parametric Study

The CST software was used to perform parametric analysis of the proposed structure. The simulation begins with T-matching feed lines and a Higgs-4 strap chip directly connected to the terminal of the dipole antenna. The antenna is loaded on both sides with U-shaped strips, which are capacitively coupled with microstrip dipole. At this stage, the reflection coefficient of the structure at the resonant frequency was -5.57 dB, with a maximum realized gain of -14.32 dB at 900 MHz, as illustrated in Figure 3(a). However, this performance was deemed insufficient for RFID implementations. Subsequently, a patch was added to the middle of the structure to enhance the realized gain and achieve a better resonance coefficient, as depicted in Figure 3(b). Although the return loss has been improved to -5.72 dB and the realized gain to -12.87 dB, the operating frequency remained far from the UHF RFID band. Next, the two vertical feed lines were extended and coupled with the patch to increase the capacitive effects on the tag antenna, enlarge the metallic surface of the patch, and shift the resonance downward, as shown in Figure 3(b). The final optimization involved tuning some important parameters of the proposed design like L_1, W_1, and L_3 as shown in Figure 1 and ensure that the antenna operates within the North American band (902 – 928 MHz).

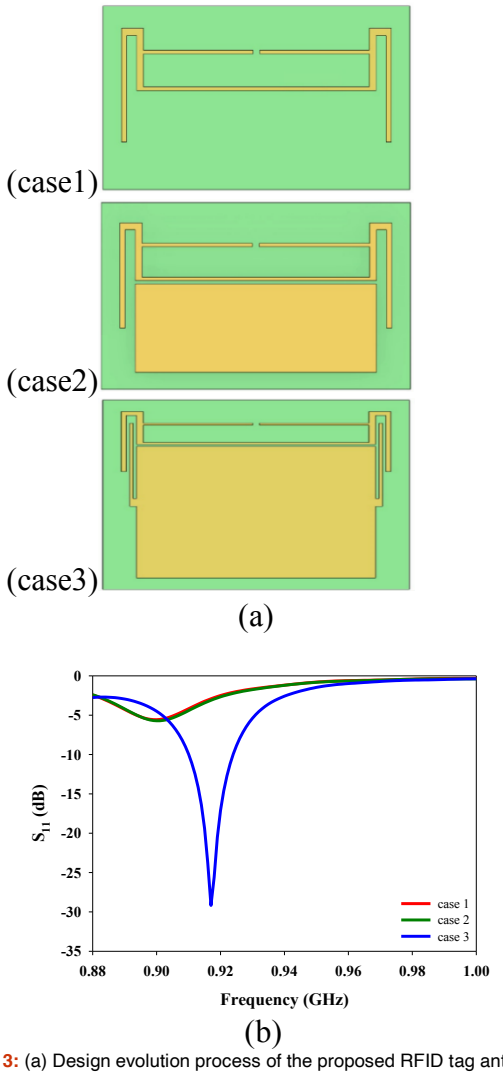

Figure 3: (a) Design evolution process of the proposed RFID tag antenna, (b) Simulated reflection coefficients of the proposed RFID tag antenna.

Simulations were conducted to investigate how variations in the length of the dipole (L_1), width of the U-shaped strip (W_1), and the length of the strip arm (L_3) affect the input impedance. It is worth nothing that when one parameter was varied, the other ones remain constant as listed in Table 1.

In Figure 3, we initially investigate the impact of the length of the dipole (L_1).

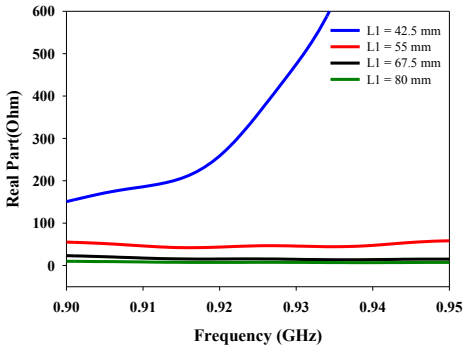

(a)

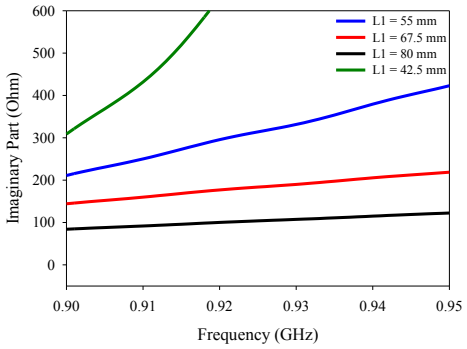

(b)

Figure 4: Simulated input impedance of the proposed RFID tag antenna for different L_1 values. (a) Real part; (b) imaginary part.

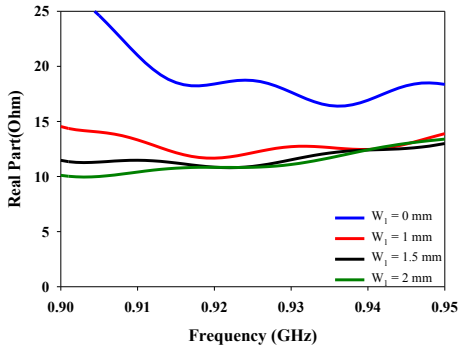

(a)

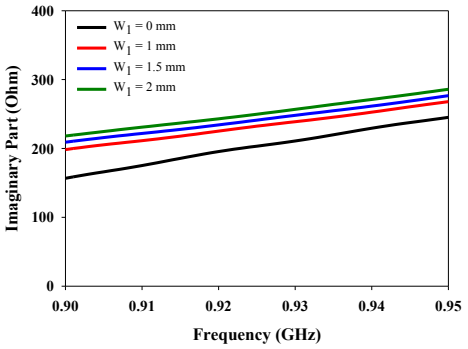

(b)

Figure 5: Simulated input impedance of the proposed RFID tag antenna for different W_1 values. (a) Real part; (b) imaginary part.

As can be seen in Figure 4, the real part of the input impedance decrease as the length L_1 goes longer from 42.5 mm to 80 mm, while the imaginary part decreases. Figure 5 shows the simulated input impedance of the proposed RFID tag antenna as a function of frequency (0.9 GHz to 0.95 GHz) for different values of W_1. The real part decreases as the width W_1 increases from 0 to 2 mm, while the imaginary part increases as the width W_1 increases from 0 to 2 mm. Furthermore, Figures 4 and 5 reveal that the parameters L_1 and W_1 can be used to tune the input impedance of the proposed tag antenna.

Figure 6 shows calculated values of real and imaginary parts of the impedance in term of frequency for different values of radiating element stub length L_3. At smaller values of L_3 (e.g. L_3=45 mm), the impedance shows a significant frequency-dependent increase, suggesting resonance behavior and stronger coupling effects. In contrast, larger values of L_3 (L_3 = 55, 65 and 75 mm) result in more stable impedance characteristics with reduced sensitivity to frequency changes. This trend highlights the stabilizing effect of increasing the radiating element size, thereby reducing reactive coupling and improving overall system consistency. Consequently, the parameter L_3 proves to be a critical design variable that enables precise tuning of impedance characteristics to meet specific operational requirements.

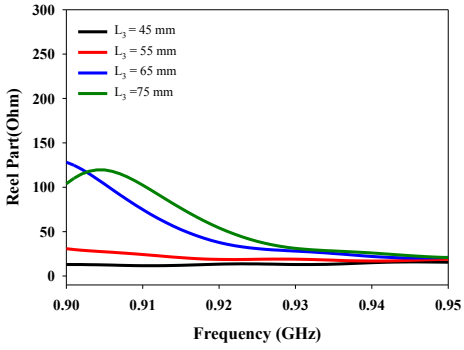

(a)

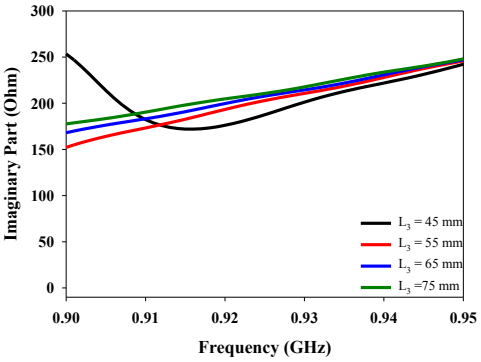

(b)

Figure 6: Simulated input impedance of the proposed RFID tag antenna for different L_3 values. (a) Real part; (b) imaginary part.

Figure 7 illustrates the effect of varying the size of the backing metallic plate on the tag's performance, especially increasing the gain. Initially, the length L_x and width L_y of the metallic plate were set to 30 cm x 30 cm, as depicted in Figure 7(b). Notably, when the size of the metallic plate is changed from 30 cm x 30 cm to 50 cm x30 cm, the maximum gain is -0.4 dB at the operating frequency, as shown in Figure 7(c), the tag's performance exhibits significant improvement in terms of gain.

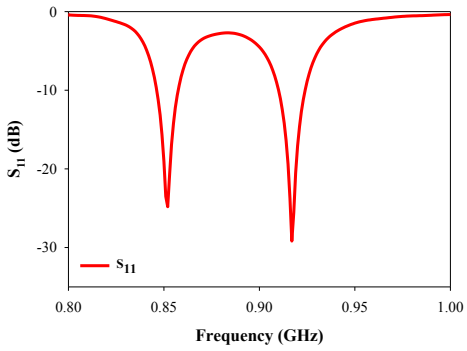

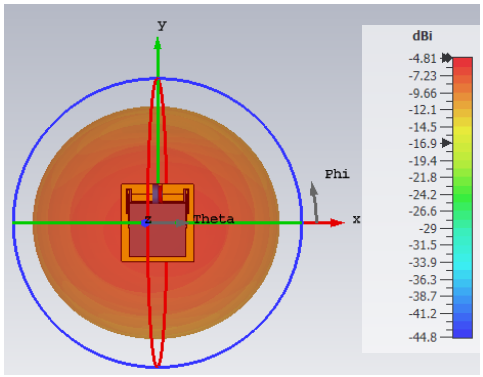

(a)

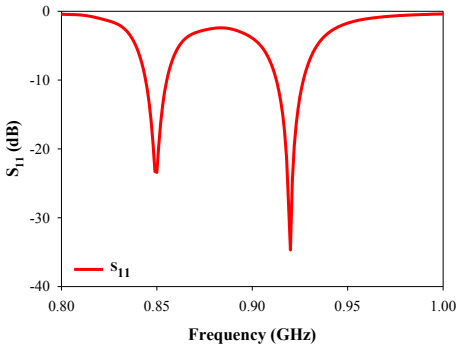

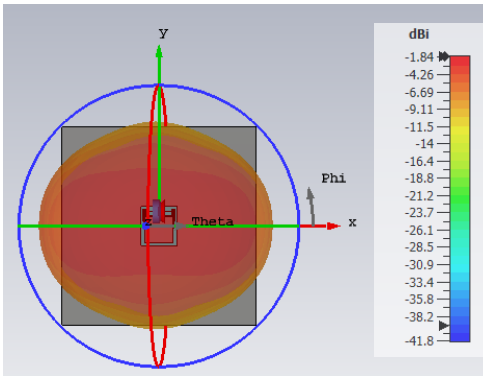

(b)

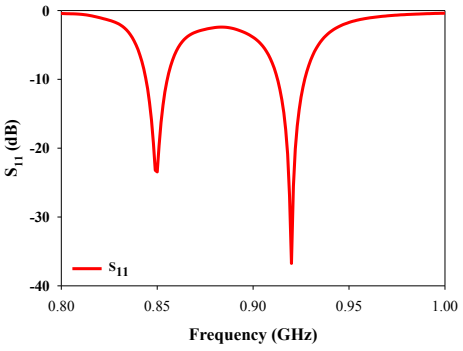

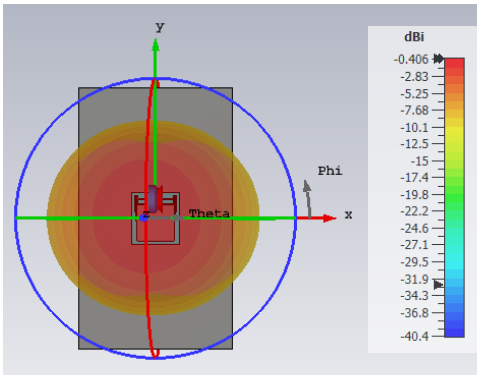

(c)

Figure 7: Simulated reflection coefficient S_{11} and realized gain of the proposed RFID tag antenna with various dimensions of metallic plate. (a) Without metallic plate; (b) 30 cm x 30 cm metallic plate; (c) 50 cm x 30 cm metallic plate.

These results indicate that the resonant frequency remains unchanged, while the gain varies with changes in the dimensions of the metallic plate. The maximum gain achieved is -0.4 dB when the dimensions of the plate are 50 cm x30 cm.

IV. Measurement Results and Discussion

A prototype of the proposed RFID tag antenna has been fabricated using an LPKF Protomat S100 with the optimized dimensions listed in Table 1 and then tested (see Figure 8) using a vector network analyzer (N5234B PNA-L network analyzer) to verify the above results. The measured input impedance of the proposed design obtained using equation (1) reported in [27] is plotted in Figure 9.

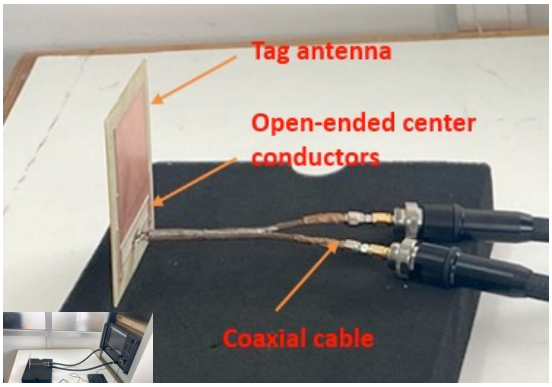

Figure 8: Experimental set-up for measuring the impedance of the fabricated tag antenna.

$$Z_d = \frac{2Z_0(1-S_{11}^2+S_{21}^2-2S_{12}^2)}{(1-S_{11})^2-S_{21}^2} \quad (1)$$

Where Z_0 is the coaxial cable's characteristic impedance.

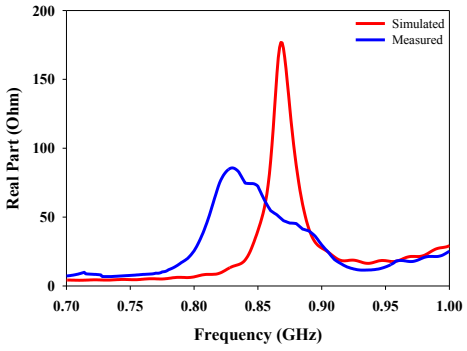

(a)

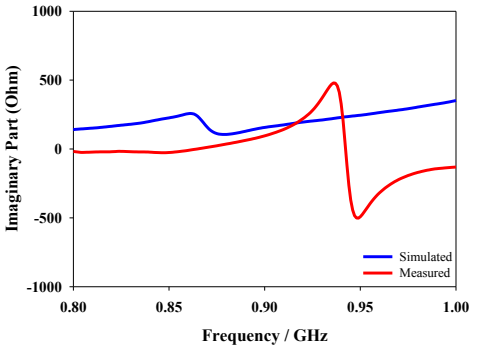

(b)

Figure 9: Simulated and measured input impedances of the proposed design in free space. (a) Real part; (b) imaginary part.

From measurement shown in Figure 9, the input impedance of the proposed antenna is 17.9+j110 Ω which is close to the impedance of the Higgs-4 (18.7+j108.8Ω) at 920MHz. This result ensures a maximum power transfer between the Chip and the antenna. A slight shift was noted between the measured and simulation resistance and reactance values. This discrepancy was found from the deformation of the antenna structure when the flexible pins of the balun probe were attached during measurement as shown in Figure 10, and including the environment factors like interference, the radiating metal surface and ground layer in this design, the conductivity of materials in vicinity of the tag and reader which also caused the resistance and reactance vary and affect the result.

Another aspect of practical significance for the RFID tag antenna is its reading range. This crucial attribute can be determined by using the Friis equation [28]:

$$r = \frac{\lambda_0}{4\pi}\sqrt{\frac{P_r G_r G_{tag} \tau}{P_{th}}} \quad (2)$$

Where λ_0 represents the wavelength in free space, $P_r = 1W$ stands for the reader's transmitted power, $G_r = 6\ dB_i$ is the reader antenna's gain, G_{tag} denotes the gain of the RFID tag antenna, and τ represents the power transmission coefficient. $P_{th} = 18\ dB_m$ corresponds to the minimum power threshold necessary to supply adequate power to the chip's sensitivity, specifically for the Higgs-4 chip. The experimental setup was established within a standard room with the aim of assessing the maximum reading range, see Figure 10. It comprises a Thing Magic Micro (M6e-M) RFID reader connected to a single circularly polarized patch antenna with a gain of 6 dBi within the frequency range of 800-1000 MHz. A 1.8-meter length of 50 Ω coaxial cable (model CNT-195-FR) connects the RFID reader to the polarized patch antenna, resulting in a 36 dB_m signal strength at 915 MHz. Consequently, the overall transmitted power amounts to roughly 4 watts EIRP (effective isotropic radiated power).

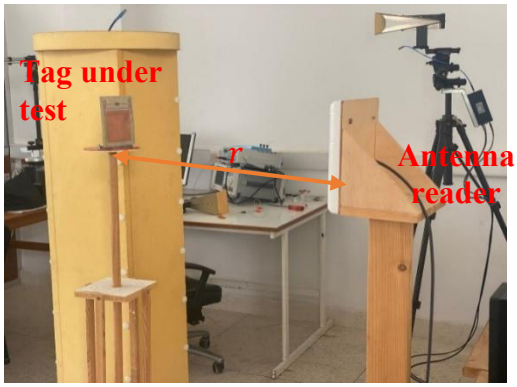

Figure 10: Measurement setup for assessing the reading range of the proposed RFID tag antenna.

To oversee the entire system, a custom software application has been installed on a computer to graphically represent the recorded activation power and reading range. The distance between the polarized patch antenna and the RFID tag antenna within this setup is set at 1 meter, ensuring that they are aligned in parallel as per the far-field requirement. It is worth noting that the measurement set-up used in this work to assess the reading range is the similar to the one presented in [29], [30]. The measured reading range of the proposed RFID tag antenna in free space is plotted in Figure 11. It can be seen that the maximum reading range is about 7 m at 920 MHz in free space. The reading range of the proposed RFID tag antenna is also measured when mounting directly on a metallic plate (without any spacing layer) measuring 50 cm × 30 cm, as depicted in Figure 11. It is evident that the presence of the metallic plate scientifically enhances the reading range performance of the proposed RFID tag antenna. The measurements results indicate that the maximum reading range for the proposed tag antenna is approximately 10.5 m at 920 MHz. Moreover, from Figure 9, it is evident that the input impedance of the RFID tag antenna remains constant whether it is placed in free space or mounted on a metallic backing plate. This feature can be attributed to the consistent maximum reading range at 920 MHz, to other RFID tag antennas published in the literature, where the resonant frequency can vary, leading to a decrease in the reading range.

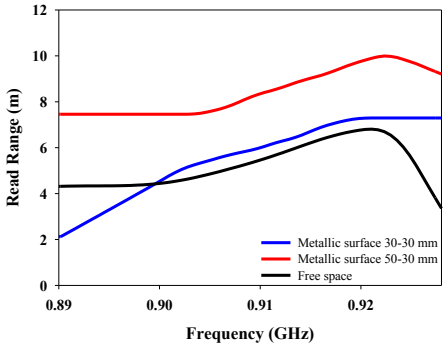

Figure 11: Measured reading range of the proposed RFID tag antenna as a function of frequency.

We have also measured the reading range of the proposed RFID tag antenna in free space using the same measurement set-up in both vertically and horizontally polarized orientations. The obtained results are depicted in Figure 12 in polar formats.

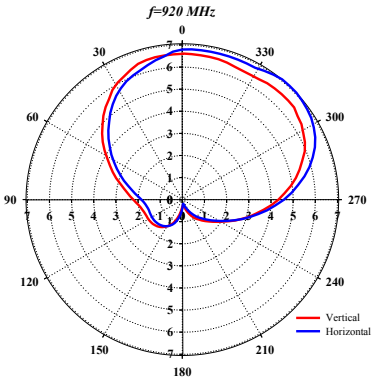

Figure 12: Measured reading range of the proposed RFID tag antenna at 920 MHz for both vertically and horizontally polarized orientations in free space.

Concerning the horizontal orientation, the measured reading range is close to 7 m in the angular ranges of $300 \leq |\theta| \leq 330°$. However, for the vertical orientation, the measured reading range is close to between 6 and 7 m in the angular ranges of $|\theta| \leq 330°$.

To get more insight about the reading range increase, we have simulated the gain of the proposed RFID tag antenna with and without a metallic plate. The obtained results are plotted in Figure 13. We can see that the gain is greater when a metallic plate is used compared to free space. This observation elucidates the reason behind the extended reading range when utilizing a metallic plate.

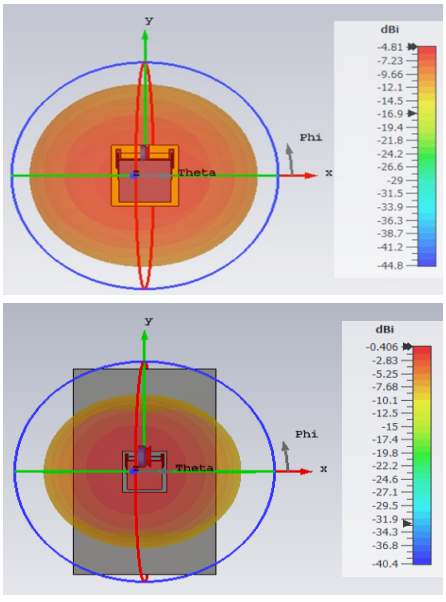

Figure 13: Simulated gain of the proposed RFID tag antenna at 920 MHz with and without metallic flat plate.

Table 2 presents a comparison between our proposed design and recently reported RFID tag antennas for metallic applications. It can be clearly seen that our proposed tag antenna has a good reading range value compared to other designs listed in Table 2. It is noteworthy that although our tag is the largest, it still achieves a commendable reading range when attached directly to a flat metallic plate measuring 50 cm × 30 cm. This is especially significant, as it remains smaller in dimension compared to other designs, which require a plate size exceeding 20 cm × 20 cm for optimal performance, which is less than ours.

Table 2: The comparison of the performance characteristic parameters of the proposed RFID tag antenna with the published works for metallic application.

Ref	Tag size (mm^3)	Metal plate Size (cm^2)	Ground	P_{th} (dBm)	Reading range (m)
[30]	28×14×3.2	20×20	yes	-15	1.8-2
[31]	41.5×55×3	20×20	yes	-18	5.12
[32]	42×50×1.6	20×20	yes	-20	5.2
[33]	55×20×1.6	40×40	yes	-18	1.8
This Work	**90×95×1.6**	**50x30**	**yes**	**-20.5**	**10.5**

V. CONCLUSION

In summary, we conducted a comprehensive numerical and experimental examination of a low-cost RFID tag antenna for metallic applications. The RFID tag antenna was meticulously designed to achieve conjugate matching with a Higg-4 chip at approximately 920 MHz, ensuring effective power transfer. Unlike traditional approaches involving via holes or shorting plates for ground connection, we proposed a T-matching configuration. This innovative design resulted in a reading range of nearly 10.5 m when the tag antenna was mounted on a 50 cm × 30 cm flat metallic plate, making it suitable for various applications such as containers tracking.

REFERENCES

[1] R. Want, “An introduction to RFID technology,” IEEE Pervasive Comput., vol. 5, no. 1, pp. 25–33, Jan./Mar. 2006.

[2] S. T. Ponis and O. K. Efthymiou, “Cloud and IoT applications in material handling automation and intralogistics,” Logistics, vol. 4, no. 3, p. 22, Sep. 2020.

[3] W. C. Tan and M. S. Sidhu, “Review of RFID and IoT integration in supply chain management,” Oper. Res. Perspect., vol. 9, no. 4, Feb. 2022, Art. no. 100229.

[4] M. El Khamlichi, A. A. Melcon, O. El Mrabet, M. A. Ennasar, and J. Hinojosa, "Flexible UHF RFID Tag for Blood Tubes Monitoring" Sensors, *vol* 19, no. 22, 2019.

[5] A. P. Sohrab, Y. Huang, M. Hussein, M. Kod, and P. Carter, ‘‘A UHF RFID tag with improved performance on liquid bottles,” IEEE Antennas Wirel. Propag. Lett, vol. 15, no. c, pp. 1673–1676, 2016.

[6] A. Sharif, J. Ouyang, Y. Yan, A. Raza, M. A. Imran and Q. H. Abbasi, "Low-Cost Inkjet-Printed RFID Tag Antenna Design for Remote Healthcare Applications," IEEE Journal Electro. RF. Micro. Med. Bio, vol. 3, no. 4, pp. 261-268, Dec. 2019.novelty

[7] M. El Khamlichi, A. A. Melcon, O. El Mrabet, M. A. Ennasar, and J. Hinojosa, "A Flexible and Low-Cost UHF RFID Tag Antenna for Blood Bag Traceability" Electronics, vol 11, no. 3, 2022.

[8] W. C. Tan and M. S. Sidhu, “Review of RFID and IoT integration in supply chain management,” Oper. Res. Perspect, vol. 9, no. 4, Feb. 2022.

[9] R. Abdulghafor, S.Turaev, H. Almohamedh, R. Alabdan, B. Almutairi, and A. Almutairi, “Recent advances in passive UHF-RFID tag antenna design for improved read range in product packaging applications: A comprehensive review,” IEEE Access, vol. 9, pp. 63611–63635, 2021,

[10] W. C. Tan and M. S. Sidhu, “Review of RFID and IoT integration in supply chain management,” Oper. Res. Perspect., vol. 9, no. 4, Feb. 2022, Art. no. 100229.

[11] L. Mo and C. Qin, “Planar UHF RFID tag antenna with open stub feed for metallic Objects,”. IEEE Trans. Antennas Propag, vol. 58, no. 9, pp. 3037-3043, June, 2010.

[12] K. Finkenzeller and D. Muller, “RFID Handbook: Fundamentals and Applications in Contactless Smart Cards, Radio Frequency Identification and Near-Field Communication, Third Edition.”.

[13] K. H. Lin, S. L. Chen, and R. Mittra, “A looped-bowtie RFID tag antenna design for metallic objects,” IEEE Trans. Antennas. Propag., vol. 61, no. 2, pp. 499–505, Feb. 2013.

[14] H. W. Son and S. H. Jeong, “Wideband RFID tag antenna for metallic surfaces using proximity-coupled feed,” IEEE Antennas Wirel. Propag. Lett., vol. 10, pp. 377–380, 2011.

[15] D. Kim and J. Yeo, “Dual-band long-range passive RFID tag antenna using an AMC ground plane,” IEEE Antennas. Trans. Propag, vol. 60, no. 6, pp. 2620–2626, Jun. 2012.

[16] H. D. Chen and Y. H. Tsao, "Low-Profile PIFA Array Antennas for UHF Band RFID Tags Mountable on Metallic Objects," in IEEE Trans. Antennas. Propag, vol. 58, no. 4, pp. 1087-1092, April 2010.

[17] W. Lan and Y. Jianguo, "A Novel UHF-RFID Tag Using a Planar Inverted-F Antenna Mountable on the Metallic Objects," 2018 IEEE Intern. Conf. Comp. Commu. Eng. Tech (CCET), Beijing, China, 2018, pp. 146-149.

[18] J. I. Tan, Y. H. Lee and E. H. Lim, "Design of a Compact On-Metal RFID Tag with a Pair of Planar Inverted-L Antennas (PILAs)," 2022 IEEE 12th Intern. Conf. RFID Tech. App (RFID-TA), Cagliari, Italy, 2022, pp. 126-127.

[19] Y. H. Lee, P. S. Chee, E. H. Lim and F. L. Bong, "Coupled-PILAs for Miniature On-metal RFID Tag Design," 2020 IEEE Asia-Pacific Micro. Conf (APMC), Hong Kong, Hong Kong, 2020, pp. 878-880.

[20] A. A. Babar, T. Bjorninen, V. A. Bhagavati, L. Sydanheimo, P. Kallio and L. Ukkonen, "Small and Flexible Metal Mountable Passive UHF RFID Tag on High-Dielectric Polymer-Ceramic Composite Substrate," in IEEE Antennas Wirel. Propag. Lett, vol. 11, pp. 1319-1322, 2012.

[21] B. Zhang et al., “Flexible anti-metal RFID tag antenna based on high conductivity graphene assembly film,” Sensors, vol. 21, no. 4, p. 1513, Feb. 2021.

[22] R. Xu and Z. Shen, "Wearable Ungrounded Tag Antenna for UHF RFID Applications," in IEEE Trans. Antennas. Propag, vol. 71, no. 4, pp. 3665-3670, April 2023.

[23] B. Gao and M. M. F. Yuen, “Passive UHF RFID packaging with electromagnetic band gap (EBG) material for metallic objects tracking,” IEEE Trans. Compon, Packag, Manuf. Tech., vol. 1, no. 8, pp. 1140–1146, Aug. 2011.

[24] L. Benmessaoud, T. P. Vuong, M .C .E. Yagoub and R. Touhami, “A novel 3-D tag with improved read range for UHF RFID localization applications”. IEEE Antennas Wirel. Propag. Lett. , vol 16, 161–164, 2017.

[25] Alien Technology, ‘‘Higgs 4 SOT,” Online, p. 4, 2014. [Online]. Available:https://www.rfid-alliance.com/RFIDshop/Alien Technology-Higgs-4-IC-Datasheet.pdf.

[26] X. Qing, C. K. Goh, and Z. N. Chen, ‘‘Impedance characterization of rfid tag antennas and application in tag co-design,” IEEE Trans. Micro. Theory Tech., vol. 57, no. 5, pp. 1268–1274, 2009.

[27] G. Marrocco, E. Di Giampaolo, and R. Aliberti, ‘‘Estimation of UHF RFID reading regions in real environments,” IEEE Antennas Propag. Mag, vol. 51, no. 6, pp. 44–57, Dec. 2009.

[28] R. Colella, L. Catarinucci, P. Coppola, and L. Tarricone, ‘‘Measurement Platform for Electromagnetic Characterization and

Performance Evaluation of UHF RFID Tags," IEEE Trans. Instrum. Meas., vol. 65, no. 4, pp. 905–914, Apr. 2016
[29] M. A. Ennasar, O. El Mrabet, K. Mohamed, and M. Essaaidi, ''Design and characterization of a broadband flexible polyimide RFID tag sensor for NaCl and sugar detection,"Prog. Electro. mag. Res. C, vol. 94, no. August,pp. 273–283, 2019
[30] J. Zhang and Y. Long, "A miniaturized via-patch loaded dual-layer RFID tag antenna for metallic object applications," IEEE Antennas Wirel. Propag. Lett. vol. 12, pp. 1184–1187, 2013.
[31] H. Li, J. Zhu, and Y. Yu, ''Compact Single-Layer RFID Tag Antenna Tolerant to Background Materials," IEEE Access, vol. 5, pp. 21070–21079, 2017.
[32] S. R. Lee, E. H. Lim, F. L. Bong, and B. K. Chung, "Slotted folded patch antenna with double-T-slots for platform-insensitive UHF tag design," IEEE Antennas. Trans. Propag., vol. 67, no. 1, pp. 670–675, Jan. 2019.
[33] Y. J. Zhang, D. Wang, and M. S. Tong, "An adjustable quarter wavelength meandered dipole antenna with slotted ground for metallically and airily mounted RFID tag," IEEE Antennas. Trans. Propag., vol. 65, no. 6, pp. 2890–2898, Jun. 2017.